



**HAL**  
open science

# Stochastic Optimization of Adaptive Cruise Control

Shangyuan Zhang, Makhlouf Hadji, Abdel Lisser, Yacine Mezali

► **To cite this version:**

Shangyuan Zhang, Makhlouf Hadji, Abdel Lisser, Yacine Mezali. Stochastic Optimization of Adaptive Cruise Control. SN Computer Science, 2022, 4 (111), 10.1007/s42979-022-01489-z . hal-03845078

**HAL Id: hal-03845078**

**<https://hal.science/hal-03845078v1>**

Submitted on 16 Oct 2023

**HAL** is a multi-disciplinary open access archive for the deposit and dissemination of scientific research documents, whether they are published or not. The documents may come from teaching and research institutions in France or abroad, or from public or private research centers.

L'archive ouverte pluridisciplinaire **HAL**, est destinée au dépôt et à la diffusion de documents scientifiques de niveau recherche, publiés ou non, émanant des établissements d'enseignement et de recherche français ou étrangers, des laboratoires publics ou privés.

# Stochastic Optimization of Adaptive Cruise Control

Shangyuan Zhang<sup>\*12</sup><sup>a</sup>, Makhlof Hadji<sup>1</sup><sup>b</sup>, Abdel Lisser<sup>2</sup><sup>c</sup> and Yacine Mezali<sup>1</sup><sup>d</sup>

<sup>1</sup>*Institut de Recherche Technologique SystemX, 8 Avenue de la Vauve, 91120 Palaiseau, France*

<sup>2</sup>*CentraleSupélec, L2S, Université Paris Saclay, 3 Rue Curie Joliot, 91190, Gif-sur-Yvette, France*  
{shangyuan.zhang, makhlof.hadji, yacine.mezali}@irt-systemx.fr, abdel.lisser@l2s.centralesupelec.fr

**Keywords:** Adaptive Cruise Control, Optimization, Stochastic Optimization, Dependence, Copula Theory.

**Abstract:** With the recent developments of autonomous vehicles, extensive studies were conducted on Adaptive Cruise Control (ACC, for short), which is an essential component of advanced driver-assistant systems (ADAS). The safety assessment must be performed on the ACC system before it goes to market. The validation process is generally conducted via simulation due to insufficient on-road data and the diversity of driving scenarios. Our paper aims to develop an optimization-based reference generation model for ACC, which can be used as a benchmark for assessment and evaluation. The model minimizes the difference between the actual and reference inter-car distance while respecting constraints about vehicle dynamics and road regulations. ACC sensors can be impacted by external factors, e.g., weather conditions and produce inaccurate data. To handle the resulting uncertainty, we propose a copula-based chance-constrained stochastic model in order to model the dependence between the random variables. Our numerical experiments show the performances of our model on randomly generated driving scenarios.

## 1 Introduction


During the past two decades, there has been an increasing trend towards autonomous driving in both industry and research, which led to many technological advances and commercial successes. Autonomous vehicle applications, e.g., advanced driver assistance systems (ADAS, for short) are extensively incorporated into modern cars to enhance safety and improve driving comfort. The most basic feature of ADAS is Adaptive Cruise Control (ACC), which has been the focus of research for several years.


### 1.1 ACC Overview


Since 1966, ACC has aimed to keep a safe distance from a leading vehicle by adjusting the vehicle's speed and acceleration (Levine and Athans, 1966). This functionality relies both on sensor information about the location and the motion of the vehicle ahead and on a controller to regulate the spacing between the vehicles. An ACC-equipped vehicle drives at a


preset speed until a leading car is detected by the sensors, then switches to the distance regulation mode by activating the ACC controller, which calculates the safety distance and controls the operation.

Various approaches are applied to achieve the objective of designing an ACC that most closely matches the human expert driving behavior in terms of maneuvering vehicle speed according to different driving conditions with respect to traffic regulations and comfortable driving. These ACC systems target different objectives and are designed under different standards. Therefore, we need a thorough validation process to ensure the safety of those ACC systems and also assess their performance before making them commercially available. The result of the validation and evaluation also allows to identify potential areas for improvement by identifying current weaknesses. Due to the fact that the costly and time-consuming real road tests cannot cover a large number of driving scenarios, we carry out the validation process within a simulator to generate the driving scenarios. The latter includes the motion state of the vehicles at each sampling time.

<sup>a</sup>  <https://orcid.org/0000-0003-0230-8618>

<sup>b</sup>  <https://orcid.org/0000-0003-1048-753X>

<sup>c</sup>  <https://orcid.org/0000-0003-1318-6679>

<sup>d</sup>  <https://orcid.org/0000-0003-1912-9093>

## 1.2 Problem Description

As part of the functional testing of ADAS, the goal of the ACC validation is to determine whether the right decision was made, a critical accident was avoided, and identify potential flaws. The validation process starts with our model, where each driving scenario serves as an input, and the reference commands are calculated by solving an optimization problem. Then, the analysis of the actual commands is performed through a comparison with our generated reference commands. This process is illustrated in Figure 1. Generating reference trajectories is a typical motion planning problem, and there are approaches to achieve this goal, e.g., sampling-based methods, graph-based methods, and optimization-based methods. Among them, the optimization approach seems the best suited to our problem as it provides more flexibility to tailor the objectives and the constraints meeting the requirements of various driving scenarios.

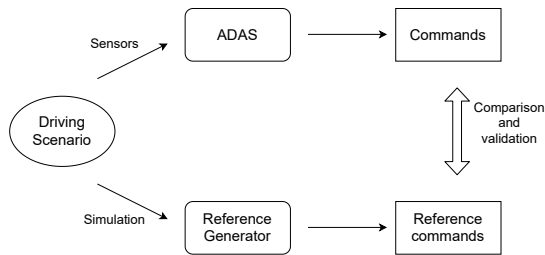


Figure 1: Validation process of ADAS

As part of an ACC system, various types of sensors may be employed, such as cameras, lidar, radar etc. Sensor performances are highly influenced by a variety of factors, including the maintenance state and the environmental conditions (Rasshofer et al., 2011). There is an inherent level of inaccuracy in sensor data which must be considered in the simulations. In order to deal with the sensor uncertainties, we study a chance-constrained stochastic programming model based on the copula theory to take into consideration the dependence of the random variables.

## 1.3 Our Contribution

The main contribution of this paper is to make an extension of previous work (Zhang et al., 2022) and study the stochastic optimization model based on copula theory for ACC reference generation. Using the optimization framework, we are able to come up with the best command to optimize the distance between two vehicles while satisfying all the

problem constraints. The copula theory in modeling uncertainty has enabled us to develop a robust and flexible model that is suitable for application in the real world. Moreover, we present a comprehensive comparison of the results obtained with our generated driving data that simulates real driving scenarios to demonstrate the benefit of the stochastic models.

## 1.4 Paper's Organization

The remainder of the paper is organized as follows. Section II discusses different ACC algorithms under study and provides a classification of the used approaches. Section III describes our ACC validation model and describes the mathematical tools used for our formulation. In Section IV, we provide numerical experiments and simulations and compare our different approaches (deterministic and stochastic). Conclusions and future work are provided in Section V.

## 2 Literature Review

### 2.1 ACC Modeling

Many ACC system problems are solved with two main approaches based on the following:

- **Optimal Control (OC) Methods:** An optimal control problem is derived from the modeling of a system and the control design of that system, which is then solved numerically and refined using methods of optimization. See (Chehardoli, 2020; Jiang et al., 2020; Kim, 2012).
- **Model Predictive Control (MPC):** These methods have been widely considered and then reached a high popularity since 2010 (see references (Chen et al., 2021; Takahama and Akasaka, 2018; Weißmann et al., 2018; Naus et al., 2010), for example). The control mechanism is based on a receding horizon approach for the online optimization process. The MPC involves predicting future system behavior and then calculating optimal control inputs to optimize the objective function.

A wide variety of papers has studied ACC from multiple perspectives, including:

- Driver behavior modeling (see for example (Varotto et al., 2020; Kummetha et al., 2020; Seppelt and Lee, 2015)). Modeling the interaction between the driver and the ACC is done by analyzing the characteristics of driver behavior

and how those characteristics are represented by state transition diagrams.

- String stability. In (Gunter et al., 2019; Makridis et al., 2020; Khound et al., 2021), ACC model string stability was assessed in order to ensure that disturbances are not amplified.
- Collision avoidance. Authors of (Lunze, 2018; Magdici and Althoff, 2017) develop a variety of objectives for ACC design that are necessary and sufficient for ensuring collision avoidance and time-headway spacing.

Our ACC reference generation model is capable of generating reference commands with optimal spacing policies and collision avoidance based on vehicle dynamics and other comfort constraints.

## 2.2 ACC Validation and Testing

Validating the functionality of autonomous driving is also an important task, not only for ACC but also for other modules which need assessments. In (Lattarulo et al., 2017), the authors present a global framework of testing methodology for the evaluation of path planning and control algorithms, including a unified test architecture and validation process. Other similar works include (Lattarulo et al., 2018), (Alnaser et al., 2019).

Aside from the overall testing framework, individual functionality like ACC should be carefully considered. In (Mehra et al., 2015), an experimental platform is presented for the validation and demonstration of an optimization-based ACC controller, whilst (Djoudi et al., 2020) presents a simulation-based toolchain for reference generation and test analysis. Several other insightful works on testing and validating adaptive cruise control can be found in (Schmied et al., 2015; Shakouri et al., 2015).

To improve the safety of an ACC system, we proposed an ACC reference generation model that can be integrated into a validation process by adapted evaluation metrics.

Moreover, and for the sake of clarity, we provide details on the comparison of our proposed approach to the closest works of the literature. They are summarized in Table 1, in which we introduced key characteristics as follows:

- **Optimization** approaches of the proposed literature are classified to be deterministic or stochastic
- Three more key characteristics qualifying ACC modeling are provided: **OC** for Optimal Control,

**MPC** for Model Predictive Control, and **QO** for Quadratic Optimization.

## 3 Problem Formulation

### 3.1 Overview

In this section, we describe the modeling of the ACC driving scenario and the formulation of the related optimization problem. A typical ACC driving scenario includes two cars driving simultaneously in a single lane, namely, the ego car and the target car. The ego car is equipped with an ACC system, whilst the target car is the leading car positioned ahead. Figure 2 illustrates the driving scenario, as well as the states of two cars at time  $t_i$ . The purpose of our ACC reference generation is to generate a sequence of acceleration commands, i.e., the decision variables in our optimization problem. The objective of the ego car is to keep a distance from the target car with respect to different constraints, e.g., vehicle dynamics, driving comfort, and road regulations.

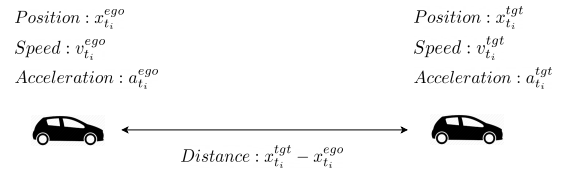


Figure 2: ACC driving scenario at moment  $t_i$ .

Suppose that the total duration of a driving scenario is  $T$  composed of  $n$  sampling time  $dt$ , i.e.  $T = ndt$  with a corresponding timestamp  $[t_0, t_1, \dots, t_i, \dots, t_n]$  where  $t_{i+1} = t_i + dt$ ,  $\forall i \in \{0, 1, \dots, n-1\}$ . At each moment  $t_i$ , the ACC of the ego car uses sensors to gather information from the target car and generates the acceleration commands. In the following, we list the parameters and the decision variable used in our model. The input parameters are given by the ego car sensors, and the decision variables represent the ACC optimal commands. The parameters of the ego car are the initial position  $x_{t_0}^{ego}$ , the initial velocity  $v_{t_0}^{ego}$  whilst the parameters of the target car are composed of the position vector  $X_T^{tgt} = (x_{t_1}^{tgt}, x_{t_2}^{tgt}, \dots, x_{t_n}^{tgt})^T$ , the velocity vector  $V_T^{tgt} = (v_{t_0}^{tgt}, v_{t_1}^{tgt}, \dots, v_{t_{n-1}}^{tgt})^T$  and the acceleration vector  $A_T^{tgt} = (a_{t_0}^{tgt}, a_{t_1}^{tgt}, \dots, a_{t_{n-1}}^{tgt})^T$  in the whole driving scenario. The decision variable is the ACC ego car acceleration commands vector  $A_T^{ego} = (a_{t_0}^{ego}, a_{t_1}^{ego}, \dots, a_{t_{n-1}}^{ego})^T$ .

Given the decision variable and the initial state of the ego car, we can derive the velocity and the position

Table 1: Benchmarking of our contribution with the state of the art

Existing works	Modeling of uncertainty	Key characteristics
(Chehardoli, 2020)	Yes	Robust OC for ACC designing
(Jiang et al., 2020)	Yes	Stochastic OC incorporating human drivers' risk-sensitivity
(Takahama and Akasaka, 2018)	No	MPC for ACC in traffic jam
(Chen et al., 2021)	No	MPC for ACC in cut-in scenarios
(Weißmann et al., 2018)	No	MPC for energy-optimal ACC
(Varotto et al., 2020)	No	Modeling of driver-ACC interaction
(Lunze, 2018)	No	ACC design focused on collision avoidance
(Lattarulo et al., 2017)	No	Framework of ACC testing
(Alnaser et al., 2019)	No	Verification of ACC in complex functional scenarios
(Mehra et al., 2015)	No	Experimental platform for validation of ACC
(Djoudi et al., 2020)	No	Functional testing of ACC with a simulation-based framework
<b>Our contribution</b>	Yes	QO for ACC reference generation

of the ego car by the equations of motion. The ego car velocity  $v_{t_{i+1}}^{ego}$  at time  $t_{i+1}$  is given by the velocity at the previous sample time  $v_{t_i}^{ego}$  and the acceleration  $a_{t_i}^{ego}$ :

$$v_{t_{i+1}}^{ego} = v_{t_i}^{ego} + a_{t_i}^{ego} dt. \quad (1)$$

The velocity for the whole driving scenario can be written in matrix form as

$$V_T^{ego} = \begin{pmatrix} v_{t_0}^{ego} \\ \vdots \\ v_{t_i}^{ego} \\ \vdots \\ v_{t_{n-1}}^{ego} \end{pmatrix} = \begin{pmatrix} v_{t_0}^{ego} \\ \vdots \\ v_{t_0}^{ego} + \sum_{k=0}^{i-1} a_{t_k}^{ego} dt \\ \vdots \\ v_{t_0}^{ego} + \sum_{k=0}^{n-2} a_{t_k}^{ego} dt \end{pmatrix} \quad (2)$$

$$= dt \mathcal{K}_u A_T^{ego} + v_{t_0}^{ego} \mathbb{1}_n,$$

where  $\mathcal{K}_u \in \mathbb{R}^{n \times n}$  and  $\mathbb{1}_n \in \mathbb{R}^{n \times 1}$

$$\mathcal{K}_u = \begin{pmatrix} 0 & 0 & 0 & \dots & 0 & 0 \\ 1 & 0 & 0 & \dots & 0 & 0 \\ 1 & 1 & 0 & \dots & 0 & 0 \\ \vdots & & & \ddots & & \vdots \\ 1 & 1 & 1 & \dots & 0 & 0 \\ 1 & 1 & 1 & \dots & 1 & 0 \end{pmatrix} \quad (3)$$

$$\mathbb{1}_n = \begin{pmatrix} 1 \\ 1 \\ \vdots \\ 1 \end{pmatrix}. \quad (4)$$

Similarly, the ego car position at time  $t_{i+1}$  is given by

$$x_{t_{i+1}}^{ego} = x_{t_i}^{ego} + v_{t_i}^{ego} dt + \frac{1}{2} a_{t_i}^{ego} dt^2. \quad (5)$$

The corresponding matrix format for all time steps

is

$$X_T^{ego} = \begin{pmatrix} x_{t_1}^{ego} \\ \vdots \\ x_{t_i}^{ego} \\ \vdots \\ x_{t_n}^{ego} \end{pmatrix} = \begin{pmatrix} x_{t_0}^{ego} + v_{t_0}^{ego} dt + \frac{1}{2} a_{t_0}^{ego} dt^2 \\ \vdots \\ x_{t_0}^{ego} + \sum_{k=0}^{i-1} v_{t_k}^{ego} dt + \frac{1}{2} \sum_{k=0}^{i-1} a_{t_k}^{ego} dt^2 \\ \vdots \\ x_{t_0}^{ego} + \sum_{k=0}^{n-1} v_{t_k}^{ego} dt + \frac{1}{2} \sum_{k=0}^{n-1} a_{t_k}^{ego} dt^2 \end{pmatrix} \quad (6)$$

$$= dt \mathcal{M}_n V_T^{ego} + \frac{1}{2} dt^2 \mathcal{M}_n A_T^{ego} + x_{t_0}^{ego} \mathbb{1}_n,$$

where  $\mathcal{M}_n \in \mathbb{R}^{n \times n}$ ,

$$\mathcal{M}_n = \begin{pmatrix} 1 & 0 & 0 & \dots & 0 \\ 1 & 1 & 0 & \dots & 0 \\ 1 & 1 & 1 & \dots & 0 \\ \vdots & & & \ddots & \vdots \\ 1 & 1 & 1 & \dots & 1 \end{pmatrix}. \quad (7)$$

We use Equation (2) to rewrite Equation (6) in terms of the initial position, the initial velocity and the acceleration vector, i.e.,

$$\begin{aligned} X_T^{ego} &= dt \mathcal{M}_n V_T^{ego} + \frac{1}{2} dt^2 \mathcal{M}_n A_T^{ego} + x_{t_0}^{ego} \mathbb{1}_n \\ &= dt \mathcal{M}_n (dt \mathcal{K}_u A_T^{ego} + v_{t_0}^{ego} \mathbb{1}_n) \\ &\quad + \frac{1}{2} dt^2 \mathcal{M}_n A_T^{ego} + x_{t_0}^{ego} \mathbb{1}_n \\ &= dt^2 (\mathcal{B}_n + \frac{1}{2} \mathcal{M}_n) A_T^{ego} + v_{t_0}^{ego} dt C_n \\ &\quad + x_{t_0}^{ego} \mathbb{1}_n, \end{aligned} \quad (8)$$

where  $\mathcal{B}_n = \mathcal{M}_n \cdot \mathcal{K}_u \in \mathbb{R}^{n \times n}$  and  $C_n = \mathcal{M}_n \cdot \mathbb{1}_n \in \mathbb{R}^{n \times 1}$ .

For the sake of clarity, we provide Table 2 to summarize the whole parameters and variables used

in our formulations.

In the following, we use the position and the velocity vector of the ego car to formulate our optimization problem.

### 3.2 Basic Results in Copula Theory

We give some basic definitions and results on copulas necessary for our modeling. We refer to (Nelsen, 2007) for more details.

**Definition 1.** A copula is the distribution function  $C : [0, 1]^K \rightarrow [0, 1]$  of some  $K$ -dimensional random vector whose marginals are uniformly distributed on  $[0, 1]$ .

**Proposition 1.** (Sklar's Theorem). For any  $K$ -dimensional distribution function  $F : \mathbb{R}^K \rightarrow [0, 1]$  with marginals  $F_1, \dots, F_K$ , there exists a copula  $C$  such that

$$\forall z \in \mathbb{R}^K, F(z) = C(F_1(z_1), \dots, F_K(z_K))$$

. If, moreover,  $F_K$  is continuous, then  $C$  is uniquely given by

$$C(u) = F(F_1^{-1}(u_1), \dots, F_K^{-1}(u_K)).$$

Otherwise,  $C$  is uniquely determined on range  $F_1 \times \dots \times \text{range } F_K$ .

The theoretical foundations for the application of copulas are given by Sklar's Theorem. Moreover, it states that every multivariate cumulative distribution function of a given random vector can be expressed in terms of both its marginals and a given copula.

To model the uncertainty of our problem, we consider the two following classes of copulas:

1. Independent (product) copula, defined by

$$C_{\Pi}(u) := \prod_{k=1}^K u_k.$$

The independent copula represents the joint distribution of independent random variables.

2. Gumbel-Hougaard family of copulas, given for  $\theta \geq 1$  by

$$C_{\theta}(u) := \exp \left\{ - \left[ \sum_{k=1}^K (-\ln u_k)^{\theta} \right]^{1/\theta} \right\}.$$

The independent copula can be seen as a special case of the Gumbel-Hougaard copula with  $\theta = 1$ .

### 3.3 Stochastic Modeling of ACC

In section 3.1 the whole parameters are deterministic, i.e., the input parameters are known in advance. However, in real-life autonomous vehicle problems,

the parameters are unknown and may include different sources of noise from external factors like weather. Results are highly dependent upon the quality of input data. Consequently, the parameters can be better modeled by random variables, which provide more robust solutions. In the following, we model the ACC problem by chance constrained problem. We suppose that the target car's position information  $x_{t_i}^{tgt}$  obtained from the ego car's sensor includes some noise and follows a normal distribution  $x_{t_i}^{tgt} \sim N(\mu_i, \sigma_i^2)$  with a joint distribution driven by the Gumbel-Hougaard copula  $C_{\theta}$  for  $\theta \geq 1$  (Cheng et al., 2015; Houda and Lisser, 2014).

In the following, we outline how the generation of the ACC reference considering uncertainty can be viewed as an optimization problem.

$$\min_{A_T^{ego}} \|QA_T^{ego} + P\| \quad (9)$$

$$\text{s.t. } dt^2(\mathcal{B}_n + \frac{1}{2}\mathcal{M}_n)A_T^{ego} \leq \hat{X}_T^{tgt} - v_{t_0}^{ego} dt C_n - (x_{t_0}^{ego} + d_s)\mathbb{1}_n, \quad (10)$$

$$- (v_{max} + v_{t_0}^{ego})\mathbb{1}_n \leq dt \mathcal{K}_u A_T^{ego} \leq (v_{max} - v_{t_0}^{ego})\mathbb{1}_n, \quad (11)$$

$$- a_{max}\mathbb{1}_n \leq A_T^{ego} \leq a_{max}\mathbb{1}_n, \quad (12)$$

$$- j_{max}dt\mathbb{1}_n \leq \mathcal{D}_n A_T^{ego} \leq j_{max}dt\mathbb{1}_n. \quad (13)$$

The following part explains in detail how we derive the objective function (9) and how constraints (10, 11, 12, 13) are developed.

The objective of ACC is to maintain a safe distance between the ego car and the target car. In order to calculate the reference distance between the ego car and the target car, we define two terms: the inter-vehicle time  $tc$  (for instance, 3 seconds) for the ego car to brake safely and the standstill distance  $\delta S$  to ensure there is always enough room between the two adjacent cars.

At each moment  $t_k$ , the reference distance of ACC in platoons is defined by

$$d_k^{ref} = (v_{t_{k-1}}^{ego} - v_{t_{k-1}}^{tgt})tc + \frac{1}{2}(a_{t_{k-1}}^{ego} - a_{t_{k-1}}^{tgt})tc^2 + \delta S. \quad (14)$$

Therefore, the reference distance vector in the whole driving scenario is :

$$\begin{aligned} D_T^{ref} &= tc(dt \mathcal{K}_u A_T^{ego} + v_{t_0}^{ego}\mathbb{1}_n - V_T^{tgt}) \\ &\quad + \frac{1}{2}tc^2(A_T^{ego} - A_T^{tgt}) + \delta S\mathbb{1}_n \\ &= (dt \cdot tc \mathcal{K}_u + \frac{1}{2}tc^2 I)A_T^{ego} - tcV_T^{tgt} \\ &\quad - \frac{1}{2}tc^2 A_T^{tgt} + (\delta S + v_{t_0}^{ego}tc)\mathbb{1}_n. \end{aligned} \quad (15)$$

Table 2: Summary of used parameters and variables in our formulations

	Symbols	Meaning
Target Car	$A_T^{tgt}$	Acceleration profile during simulation
	$a_{t_i}^{tgt}$	Acceleration at time $t_i$
	$V_T^{tgt}$	Speed profile during simulation
	$v_{t_i}^{tgt}$	Speed at time $t_i$
	$X_T^{tgt}$	Position profile during simulation
	$x_{t_i}^{tgt}$	Position at time $t_i$
Ego Car	$A_T^{ego}$	Acceleration profile during simulation
	$a_{t_i}^{ego}$	Acceleration at time $t_i$
	$V_T^{ego}$	Speed profile during simulation
	$v_{t_i}^{ego}$	Speed at time $t_i$
	$X_T^{ego}$	Position profile during simulation
	$x_{t_i}^{ego}$	Position at time $t_i$
	$J_T^{ego}$	Jerk profile during simulation
	$j_{t_i}^{ego}$	Jerk at time $t_i$
Other Parameters	$Q$	Matrix of size $n \times n$
	$P$	Vector of size $n$

Moreover, if we consider the position of the target car  $X_T^{tgt}$  to be its mean value  $\mu_T = (\mu_1, \mu_2, \dots, \mu_n)^T$ , the current distance between the ego car and the target car is

$$\begin{aligned} D_T^{vehicle} &= \mu_T - X_T^{ego} \\ &= \mu_T - [dt^2(\mathcal{B}_n + \frac{1}{2}\mathcal{M}_n)A_T^{ego} \\ &\quad + v_{t_0}^{ego} dt C_n + x_{t_0}^{ego} \mathbb{1}_n]. \end{aligned} \quad (16)$$

By combining (16) and (15), we obtain the objective function (9):

$$\begin{aligned} &\min_{A_T^{ego}} \|D_T^{vehicle} - D_T^{ref}\| \\ &= \min_{A_T^{ego}} \|\mu_T - [dt^2(\mathcal{B}_n + \frac{1}{2}\mathcal{M}_n)A_T^{ego} \\ &\quad + v_{t_0}^{ego} dt C_n + x_{t_0}^{ego} \mathbb{1}_n] - [(dt \cdot tc \mathcal{K}_u + \frac{1}{2}tc^2 I)A_T^{ego} \\ &\quad - tcV_T^{tgt} - \frac{1}{2}tc^2 A_T^{tgt} + (\delta S + v_{t_0}^{ego} tc) \mathbb{1}_n]\| \\ &= \min_{A_T^{ego}} \|\underbrace{-(dt^2 \mathcal{B}_n + \frac{1}{2}dt^2 \mathcal{M}_n + dt \cdot tc \mathcal{K}_u} \\ &\quad + \frac{1}{2}tc^2 I)A_T^{ego} + \mu_T + tcV_T^{tgt} + \frac{1}{2}tc^2 A_T^{tgt} - \delta S \mathbb{1}_n \\ &\quad - v_{t_0}^{ego} tc \mathbb{1}_n - x_{t_0}^{ego} \mathbb{1}_n - v_{t_0}^{ego} dt C_n\| \\ &= \min_{A_T^{ego}} \|QA_T^{ego} + P\|, \end{aligned} \quad (17)$$

where  $Q = -(dt^2 \mathcal{B}_n + \frac{1}{2}dt^2 \mathcal{M}_n + dt \cdot tc \mathcal{K}_u + \frac{1}{2}tc^2 I)$ ,  $P = \mu_T + tcV_T^{tgt} + \frac{1}{2}tc^2 A_T^{tgt} - \delta S \mathbb{1}_n - v_{t_0}^{ego} tc \mathbb{1}_n - x_{t_0}^{ego} \mathbb{1}_n - v_{t_0}^{ego} dt C_n$  and  $\|\cdot\|$  is the Euclidean norm.

In addition to the objective function (9), we detail the above-mentioned constraints:

- Constraint (10) is the minimum distance constraint that aims to prevent the vehicles collisions, where

$$\hat{X}_T^{tgt} = \begin{pmatrix} \mu_1 + \sigma_1 F_N^{-1}(1 - \alpha^{z_{t_1}^{1/\theta}}) \\ \mu_2 + \sigma_2 F_N^{-1}(1 - \alpha^{z_{t_2}^{1/\theta}}) \\ \vdots \\ \mu_n + \sigma_n F_N^{-1}(1 - \alpha^{z_{t_n}^{1/\theta}}) \end{pmatrix}, \quad (18)$$

and

$$\sum_{t_i} z_{t_i} = 1, \quad z_{t_i} \geq 0, \quad \forall t_i,$$

where  $F_N^{-1}$  is the inverse of the standard normal cumulative distribution function.

This constraint results from the following chance constraint with a given threshold  $\alpha$  (Prékopa, 2013):

$$\mathbb{P}(D_{t_i}^{vehicle} \geq d_s, \forall t_i) \geq \alpha. \quad (19)$$

- Constraint (11) is the maximum velocity constraint. Routes typically have a maximum velocity limit which leads to the velocity constraint. For a given speed limit  $v_{max}$ , the constraint is deduced from

$$\|V_T^{ego}\|_{\infty} \leq v_{max}. \quad (20)$$

- Constraint (12) is the maximum acceleration constraint. Car passengers' comfort is impacted by acceleration. Vehicle maneuverings like rapid

acceleration or braking should be avoided. Our model proposes an acceleration limit of  $a_{max}$  based on this motivation.

$$\|A_T^{ego}\|_\infty \leq a_{max}. \quad (21)$$

- Constraint (13) is the maximum jerk constraint. In jerk, we measure the acceleration variances, which significantly affect the comfort level of passengers. A maximum limit  $j_{max}$  is required for this constraint.

$$\|J_T^{ego}\|_\infty \leq j_{max} \quad (22)$$

Since  $j_i = (a_i^{ego} - a_{i-1}^{ego})/dt$ , the jerk constraint can be simplified to (13) where  $\mathcal{D}_n \in \mathcal{R}^{n \times n}$  is given by

$$\mathcal{D}_n = \begin{pmatrix} 1 & 0 & 0 & \dots & 0 & 0 \\ -1 & 1 & 0 & \dots & 0 & 0 \\ 0 & -1 & 1 & \dots & 0 & 0 \\ \vdots & & & \ddots & \vdots & \\ 0 & 0 & 0 & \dots & 1 & 0 \\ 0 & 0 & 0 & \dots & -1 & 1 \end{pmatrix}. \quad (23)$$

To prove the equivalence between (10) and (19), we define two variables:

$$\xi_{t_i} := -\frac{x_i^{igt} - \mu_i}{\sigma_i},$$

$$b_{t_i} := -\frac{x_i^{ego} + d_s - \mu_i}{\sigma_i}.$$

It's easy to see that  $\xi_{t_i}$  follows a standard normal distribution.

**Lemma 1.** *If the random vector  $(\xi_{t_1}, \dots, \xi_{t_n})^T$  has a joint distribution driven by the Gumbel-Hougaard copula  $C_\theta$  with some  $\theta \geq 1$ , then the constraint  $\mathbb{P}(D_{t_i}^{vehicle} \geq d_s, \forall t_i) \geq \alpha$  is equivalent to*

$$x_{t_i}^{ego} + d_s - \mu_i - \sigma_i F_N^{-1}(1 - \alpha^{z_{t_i}^{1/\theta}}) \leq 0, \quad \forall t_i, \quad (24)$$

$$\sum_{t_i} z_{t_i} = 1, \quad z_{t_i} \geq 0, \quad \forall t_i.$$

*Proof.* In one direction, we need to prove if  $\mathbb{P}(D_{t_i}^{vehicle} \geq d_s, \forall t_i) \geq \alpha$  is true, then we can find a group of  $z_{t_i}$  such that (24) holds true.

The inequality (24) is equivalent to

$$\frac{x_{t_i}^{ego} + d_s - \mu_i}{\sigma_i} \leq F_N^{-1}(1 - \alpha^{z_{t_i}^{1/\theta}}), \quad \forall t_i, \quad (25)$$

namely,

$$F_N(b_{t_i}) \geq \alpha^{z_{t_i}^{1/\theta}}. \quad (26)$$

We define  $\tilde{z}_{t_i} := \left(\frac{\ln F_N(b_{t_i})}{\ln \alpha}\right)^\theta$ , for  $i = 1, \dots, n$ .

And  $z_{t_i} := \frac{\tilde{z}_{t_i}}{\sum_{i=1}^n \tilde{z}_{t_i}}$ , for  $k = 1, \dots, n$ .

It's easy to verify that  $z_{t_i}$  satisfies  $\sum_{t_i} z_{t_i} = 1, z_{t_i} \geq 0$ . Since  $\tilde{z}_{t_i} := \left(\frac{\ln F_N(b_{t_i})}{\ln \alpha}\right)^\theta$ , then we have  $F_N^{-1}(\alpha^{\tilde{z}_{t_i}^{1/\theta}}) = b_{t_i}, \forall t_i$ . Moreover, as

$$\begin{aligned} & \mathbb{P}(D_{t_i}^{vehicle} \geq d_s, \forall t_i) \\ &= \mathbb{P}(\xi_{t_i} \leq b_{t_i}, \forall t_i) \\ &= C_\theta(F_N(b_{t_1}), \dots, F_N(b_{t_n})) \\ &= C_\theta(F_N(\alpha^{\tilde{z}_{t_1}^{1/\theta}}), \dots, F_N(\alpha^{\tilde{z}_{t_n}^{1/\theta}})) \\ &= \exp\left\{-\left[\sum_{t_i} \left(-\ln \alpha^{\tilde{z}_{t_i}^{1/\theta}}\right)^\theta\right]^{1/\theta}\right\} \\ &= \alpha^{[\sum_{i=1}^n \tilde{z}_{t_i}]^{1/\theta}}, \end{aligned} \quad (27)$$

and  $\mathbb{P}(D_{t_i}^{vehicle} \geq d_s, \forall t_i) \geq \alpha$  with  $\alpha < 1$ . We have  $[\sum_{i=1}^n \tilde{z}_{t_i}]^{1/\theta} \leq 1$  and further  $\sum_{i=1}^n \tilde{z}_{t_i} \leq 1$ , then we have  $z_{t_i} \geq \tilde{z}_{t_i}, \forall t_i$ . Therefore,  $F_N^{-1}(\alpha^{z_{t_i}^{1/\theta}}) \leq b_{t_i}, \forall t_i$ , which means  $z_k$  satisfies (24).

For another direction, if (24) holds true, from the definition of the Gumbel-Hougaard copula and Sklar's theorem, we have

$$\begin{aligned} & \mathbb{P}(D_{t_i}^{vehicle} \geq d_s, \forall t_i) \\ &= \mathbb{P}(\xi_{t_i} \leq b_{t_i}, \forall t_i) \\ &= C_\theta(F_N(b_{t_1}), \dots, F_N(b_{t_n})) \\ &\geq C_\theta\left(\alpha^{z_{t_1}^{1/\theta}}, \dots, \alpha^{z_{t_n}^{1/\theta}}\right) \\ &= \exp\left\{-\left[\sum_{t_i} \left(-\ln \alpha^{z_{t_i}^{1/\theta}}\right)^\theta\right]^{1/\theta}\right\} \\ &= \exp\left\{-\left[\sum_{t_i} \left(-z_{t_i}^{1/\theta} \ln \alpha\right)^\theta\right]^{1/\theta}\right\} \\ &= \exp\left\{\ln \alpha \left[\sum_{t_i} z_{t_i}\right]^{1/\theta}\right\} \\ &= \alpha. \end{aligned} \quad (28)$$

□

With Lemma 1, we prove that (10) and (19) are equivalent, thus formulating the optimization problem for ACC in the presence of uncertainty.

In addition to using our model for ACC with dependent random variables, we can also extend it to other models. By taking  $\theta = 1$ , the Gumbel-Hougaard copula is equivalent to the independent copula where the sensor's uncertainties are uncorrelated. Moreover, if we do not account for the uncertainty of the sensor error, then we can also replace the chance constraint



$\mathbb{P}(D_{t_i}^{vehicle} \geq d_s, \forall t_i) \geq \alpha$  with a normal constraint  $D_{t_i}^{vehicle} \geq d_s$ , which leads to a deterministic model of our optimization problem.

## 4 Numerical experiments

The purpose of our numerical simulations is to demonstrate the feasibility and effectiveness of our models. Firstly, we compare the deterministic and stochastic models on different randomly generated instances. The deterministic model does not consider the sensor uncertainties, whilst the stochastic model takes uncertainty into account with chance constraints. The random variables dependence is modeled by Gumbel-Hougaard copula with  $\theta = 2$ . Next, we choose five random driving scenarios and run our model with different values of the parameter  $\theta$ . The driving scenarios are generated with different configurations, including the target car's trajectory profile, the ego car's initial state and the sensor error for the ego car. Based on those generated scenarios, we formulate the optimization problem and use optimization solvers to obtain the results (Goldfarb and Idnani, 1983; Beal et al., 2018).

In order to create an ACC driving scenario, we need two types of parameters: the parameters related to the environment and to the vehicles. The parameters related to the environment include the simulation configuration and vehicle regulations, e.g., the total scenario duration, velocity limit, collision avoidance limit, etc. Those parameters reflect the real-life driving rules and simulation setting. Therefore, they are fixed during numerical experiments. The parameters related to the vehicles, e.g., initial position, velocity and distance, vary in each randomly generated instance due to the diversity of driving scenarios. In order to simulate real driving situations, the relationship among randomly generated vehicle parameters should be based on Newton's laws.

Parameters setup for numerical simulations are summarized in the sequel:

- Parameters related to the environment
  - Total duration of a scenario  $T$ :  $2s$ .
  - Sampling time step  $dt$ :  $0.05s$ .
  - Inter-vehicle time  $t_c$ :  $3s$ .
  - Standstill distance  $\sigma S$ :  $3m$ .
  - Minimum security distance  $d_s$ :  $10m$ .
  - Maximum velocity  $v_{max}$ :  $30m/s$ .
  - Maximum acceleration  $a_{max}$ :  $5m/s^2$ .
  - Maximum jerk  $j_{max}$ :  $5m/s^3$ .

– Confidence level  $\alpha$ :  $0.95$ .

- Parameters related to the vehicles

- Acceleration of the target car: independent random variables following a normal distribution with mean 0 and standard deviation 2, truncated from  $-5$  to  $5$ .
- Initial speed of target car and ego car: independent random variables following a normal distribution with mean 15 and standard deviation 10, truncated from 5 to 25.
- Standard deviation of target car position  $\sigma$ : 1.
- Initial position of target car: random variable following a normal distribution with mean 200 and standard deviation 1.
- Speed and position of target car: random variables following normal distributions with a mean calculated by an initial value and the acceleration vector, and standard deviation 1.
- Initial position of ego car: the initial position of the target car minus a random variable following a normal distribution with mean 100 and standard deviation 20, truncated from 50 to 150.

With the above-mentioned configuration, we generate 100 random driving scenarios, which are solved by the solvers both for the deterministic and stochastic models. Since the input parameters of the model are based on biased sensor data, it is possible that the result will violate the constraints (19) during the driving scenario. Hence, we measure the performances of our model through the feasibility of the solutions for different scenarios.

Amongst 100 test-driving scenario cases, we notice that only 40% of the instances are feasible for the deterministic optimal solution, whilst 71% are feasible for the stochastic optimal solution with confidence level  $\alpha = 0.95$  and  $\theta = 2$ .

For an in-depth analysis of constraint violations across 100 test driving scenarios, Figure 3 visualizes the constraint violation value  $d_s - D_T^{vehicle} \mathbb{1}_n$ , adapted from constraint (19), for the whole results of the two models. Figures 3(a) and 3(b) show the constraint violation value for the whole constraints, whilst Figures 3(c) and 3(d) show a zoom-in on a subset of constraints for better readability. In Figure 3, each curve with a different color displays the constraint violation values of a driving scenario result, and the  $x$ -axis represents the index of constraints. If the value at constraint index  $i$  exceeds 0, it means that  $d_s > D_{t_i}^{vehicle}$ , i.e. the constraint (19) is violated at this sampling time. Figure 3 clearly indicates that the stochastic model produces fewer violations than the deterministic one. Following the visualization

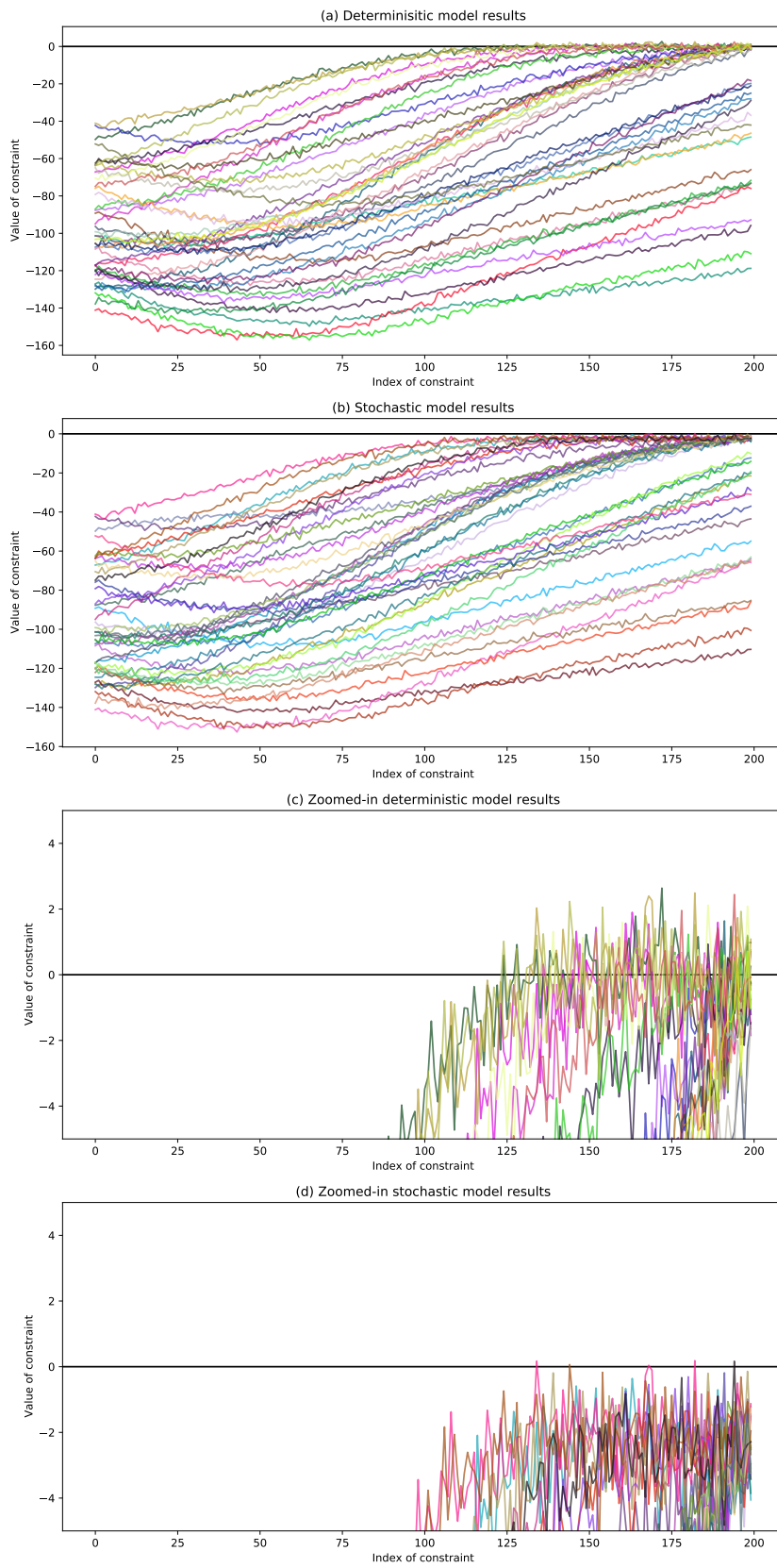


Figure 3: Constraint function values of all instances for deterministic and stochastic models.

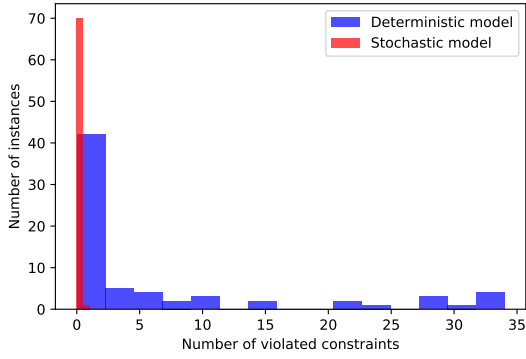


Figure 4: Histogram and cumulative histogram of the number of violated constraints for two models.

of the result, we also conduct a statistical analysis of the distribution of the violated constraints number in Figure 4. We observe that the stochastic model not only produces more feasible solutions with 0 violations but also yields fewer violations for cases where the solution is unfeasible, i.e., only a few constraints are slightly violated.

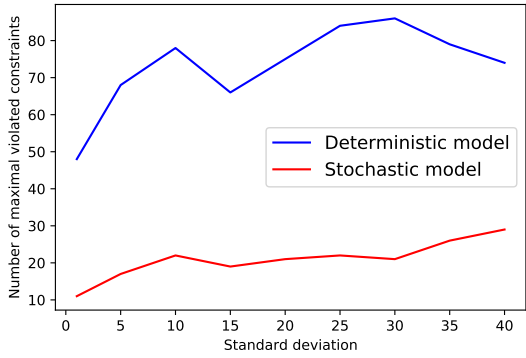


Figure 5: Maximal violated constraints under different standard deviations.

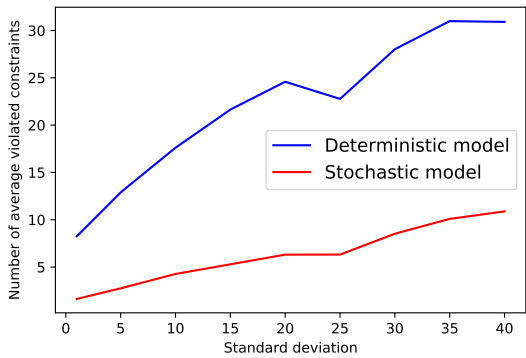


Figure 6: Average violated constraints under different standard deviations.

Furthermore, keeping all other parameters

Table 3: Summary of results.

$\theta$ \ No.	1	2	3	4	5
1	158.09	365.86	244.21	289.94	483.45
2	149.04	371.16	285.35	286.42	481.33
4	143.65	370.45	235.49	284.41	480.13
8	140.63	336.79	233.72	283.32	479.48
16	139.02	321.77	232.78	282.74	479.13

unchanged, we vary the standard deviation of the target car position, which depends on the sensor's precision, from 1 to 40 to compare the performances of each model. The value of the standard deviation is gradually increased. We consider 100 tests for each value and count the maximal and mean constraint violations for each model. In order to take a step further in our analysis, we run our model with  $\theta = 1$ . As shown in Figure 5 and Figure 6, the stochastic model always outperforms the deterministic model by producing fewer constraint violations.

In Table 3, the objective values of five driving scenarios under different configurations are presented. Each column represents the results of a generated driving scenario instance.  $\theta$  is set between 1, 2, 4, 8, 16 in order to test the robustness of our model when the dependence parameter increases.

## 5 Conclusion and future work

In this paper, we studied an optimization-based approach for ACC reference generation, taking into account the uncertainty associated with sensor information. Uncertainty is modeled by random variables, and their dependence is handled with copulas.

As a benchmark for ACC system decision making, our optimization approach can generate a reference that meets the needs of safety, comfort, and effectiveness. According to a statistical analysis of the simulation results, our chance-constrained based stochastic model can produce more robust solutions.

For future work, we propose three open research challenges that have the merit to be addressed: the development of an increasingly sophisticated vehicle model, the modeling of uncertainty by other frameworks, and the formulation of objectives that involve penalties for undesired behavior. Furthermore, we will use this optimization-based reference generation framework for other autonomous driving functions, e.g., lane keeping assistance (LKA) and collision avoidance.

## 6 Declarations

**Conflict of interest** The authors declare that they have no conflict of interest.

## REFERENCES

- Alnaser, A. J., Akbas, M. I., Sargolzaei, A., and Razdan, R. (2019). Autonomous vehicles scenario testing framework and model of computation. *SAE International Journal of Connected and Automated Vehicles*, 2(4).
- Beal, L., Hill, D., Martin, R., and Hedengren, J. (2018). Gekko optimization suite. *Processes*, 6(8):106.
- Chehardoli, H. (2020). Robust optimal control and identification of adaptive cruise control systems in the presence of time delay and parameter uncertainties. *Journal of Vibration and Control*, 26(17-18):1590–1601.
- Chen, C., Guo, J., Guo, C., Chen, C., Zhang, Y., and Wang, J. (2021). Adaptive cruise control for cut-in scenarios based on model predictive control algorithm. *Applied Sciences*, 11(11):5293.
- Cheng, J., Houda, M., and Lissner, A. (2015). Chance constrained 0–1 quadratic programs using copulas. *Optimization Letters*, 9(7):1283–1295.
- Djoudi, A., Coquelin, L., and Regnier, R. (2020). A simulation-based framework for functional testing of automated driving controllers. In *2020 IEEE 23rd International Conference on Intelligent Transportation Systems (ITSC)*, pages 1–6. IEEE.
- Goldfarb, D. and Idnani, A. (1983). A numerically stable dual method for solving strictly convex quadratic programs. *Mathematical programming*, 27(1):1–33.
- Gunter, G., Janssen, C., Barbour, W., Stern, R. E., and Work, D. B. (2019). Model-based string stability of adaptive cruise control systems using field data. *IEEE Transactions on Intelligent Vehicles*, 5(1):90–99.
- Houda, M. and Lissner, A. (2014). Archimedean copulas in joint chance-constrained programming. In *International Conference on Operations Research and Enterprise Systems*, pages 126–139. Springer.
- Jiang, J., Ding, F., Zhou, Y., Wu, J., and Tan, H. (2020). A personalized human drivers' risk sensitive characteristics depicting stochastic optimal control algorithm for adaptive cruise control. *IEEE Access*, 8:145056–145066.
- Khound, P., Will, P., and Gronwald, F. (2021). Design methodology to derive over-damped string stable adaptive cruise control systems. *IEEE Transactions on Intelligent Vehicles*, 7(1):32–44.
- Kim, S. (2012). *Design of the adaptive cruise control systems: An optimal control approach*. PhD thesis, UC Berkeley.
- Kummetha, V. C., Kondyli, A., and Schrock, S. D. (2020). Analysis of the effects of adaptive cruise control on driver behavior and awareness using a driving simulator. *Journal of Transportation Safety & Security*, 12(5):587–610.
- Lattarulo, R., Heß, D., Matute, J. A., and Perez, J. (2018). Towards conformant models of automated electric vehicles. In *2018 IEEE International Conference on Vehicular Electronics and Safety (ICVES)*, pages 1–6. IEEE.
- Lattarulo, R., Pérez, J., and Dendaluze, M. (2017). A complete framework for developing and testing automated driving controllers. *IFAC-PapersOnLine*, 50(1):258–263.
- Levine, W. and Athans, M. (1966). On the optimal error regulation of a string of moving vehicles. *IEEE Transactions on Automatic Control*, 11(3):355–361.
- Lunze, J. (2018). Adaptive cruise control with guaranteed collision avoidance. *IEEE Transactions on Intelligent Transportation Systems*, 20(5):1897–1907.
- Magdici, S. and Althoff, M. (2017). Adaptive cruise control with safety guarantees for autonomous vehicles. *IFAC-PapersOnLine*, 50(1):5774–5781.
- Makridis, M., Mattas, K., Ciuffo, B., Re, F., Kriston, A., Minarini, F., and Rognelund, G. (2020). Empirical study on the properties of adaptive cruise control systems and their impact on traffic flow and string stability. *Transportation research record*, 2674(4):471–484.
- Mehra, A., Ma, W.-L., Berg, F., Tabuada, P., Grizzle, J. W., and Ames, A. D. (2015). Adaptive cruise control: Experimental validation of advanced controllers on scale-model cars. In *2015 American Control Conference (ACC)*, pages 1411–1418. IEEE.
- Naus, G., Ploeg, J., Van de Molengraft, M., Heemels, W., and Steinbuch, M. (2010). Design and implementation of parameterized adaptive cruise control: An explicit model predictive control approach. *Control Engineering Practice*, 18(8):882–892.
- Nelsen, R. B. (2007). *An introduction to copulas*. Springer Science & Business Media.
- Prékopa, A. (2013). *Stochastic programming*, volume 324. Springer Science & Business Media.
- Rasshofer, R. H., Spies, M., and Spies, H. (2011). Influences of weather phenomena on automotive laser radar systems. *Advances in Radio Science*, 9(B. 2):49–60.
- Schmied, R., Waschl, H., and Del Re, L. (2015). Extension and experimental validation of fuel efficient predictive adaptive cruise control. In *2015 American Control Conference (ACC)*, pages 4753–4758. IEEE.
- Seppelt, B. D. and Lee, J. D. (2015). Modeling driver response to imperfect vehicle control automation. *Procedia Manufacturing*, 3:2621–2628.
- Shakouri, P., Czczot, J., and Ordys, A. (2015). Simulation validation of three nonlinear model-based controllers in the adaptive cruise control system. *Journal of Intelligent & Robotic Systems*, 80(2):207–229.
- Takahama, T. and Akasaka, D. (2018). Model predictive control approach to design practical adaptive cruise control for traffic jam. *International journal of automotive engineering*, 9(3):99–104.

- Varotto, S. F., Farah, H., Bogenberger, K., van Arem, B., and Hoogendoorn, S. P. (2020). Adaptations in driver behaviour characteristics during control transitions from full-range adaptive cruise control to manual driving: an on-road study. *Transportmetrica A: transport science*, 16(3):776–806.
- Weißmann, A., Görge, D., and Lin, X. (2018). Energy-optimal adaptive cruise control combining model predictive control and dynamic programming. *Control Engineering Practice*, 72:125–137.
- Zhang, S., Hadji, M., Lissner, A., and Mezali, Y. (2022). Optimization of adaptive cruise control under uncertainty. In *International Conference on Operations Research and Enterprise Systems (ICORES)*.